IOSR Journal of Applied Chemistry (IOSR-JAC)
e-ISSN: 2278-5736.Volume 18, Issue 8 Ser. I (August. 2025), PP 56-66
www.iosrjournals.org

Green Synthesis And Characterization Of Irish Potato Peels Powder–Nano-Silica Composite For Rhodamine Blue Removal

Joseph Mutie[1], Joel Mwangi[1] And Ombaka Ochieng[1]
Department Of Physical Sciences, Chuka University, P. O. Box 109-60400, Chuka

Abstract
The largest part of earth is covered by water. However, safe water for drinking has become a real challenge in everyday life. Dyes and pharmaceuticals constitute many pollutants that are either directly or indirectly discharged into water bodies water unfit for human use. To reclaim precious water resources, there are a number of technologies that are in use. Adsorption on activated carbons is commonly applied in wastewater treatment, but the high cost of activated carbon limit the use of this technique. Agricultural waste materials are currently inefficiently utilized and could be transformed into valuable adsorbents like composites. However, most composite materials are not well distributed and that's why this study focused on utilizing Irish potatoes peels powder (IPPP) and rice husk nano silica (RHNS) to synthesize Irish potatoes peels powder-nano silica composite (IPPP-NSC). To characterize the composite, powder X-ray diffraction (XRD) was used to determine the structural properties, and N_2 sorption the Brunauer-Emmett-Teller (BET) and Barrett-Joyner-Halenda (BJH) methods to determine the textural properties. The adsorption capacity of RB blue by the composite was optimum at pH 4, adsorbent dosage 0.1g, initial concentration 1mg/l and agitation speed of 240 rpm. The removal efficiency of the composite was found to be 97.57% for RB. RB removal best fitted Freundlich isotherm in the composite adsorbent used with R^2=0.996. Kinetic data fitted pseudo-second-order (R^2 =0.9989 for RB) which was more suitable in explaining the adsorption rate.

Keywords: *Rhodamine Blue, adsorbent, nanotechnology, characterization and degradation.*

Date of Submission: 18-08-2025 Date of Acceptance: 28-08-2025

I. Introduction

The invention of new technologies and increase in population of mankind, has had great impact on the quality of water. Among the consequences of this rapid growth is environmental disorder with a big pollution problem. Water pollution is a global concern and therefore scientists are coming up with different ways to address this menace (Schwarzenbach *et al*., 2010). Removing pollutants from water is the crying need of the hour and developing a cost effective and environmentally safe method to achieve the same is a challenging task.

Industrialization has caused major damages due to huge amount of wastewater generated from factories that contain toxic wastes such as heavy metals and color. Most of unspent dyes generate undesirable effluents and are usually discharged to the environment without treatment (Dasgupta *et al*., 2015). The release of dyes into water by industries is undesirable and cause serious environmental problem. It contains various organic compounds and toxic substances which are hazardous and harmful to aquatic organisms (Robinson *et al*., 2001).

The use and discharge of synthetic dyes from textile, food, printing and ink, paper and plastics industries are an environmental health concern, especially to developing countries (Chequer *et al*., 2011). Dyes not only affect aesthetic merit but also affect aquatic ecosystems, reducing light penetration for photosynthesis, and gas dissolution in lakes, rivers and other water bodies (Saratale *et al*., 2011 and Modi *et al*., 2010). Most of these dyes have been shown to cause allergy, dermatitis, skin irritation and intestinal cancer to humans (Golka *et al*., 2004). In addition, some dyes are either toxic or mutagenic and carcinogenic (Benson *et al*., 1980). Without adequate treatment these dyes are persistent in the environment and hence pose a serious threat to survival of both terrestrial and aquatic ecosystems (Da Silva *et al*., 2011 and Carneiro *et al*., 2010). This study focused on removal of Rhodamine blue (RB) from waste waters.

II. Materials And Methods

All reagents used were purchased from sigma Aldrich and used as provided without purification and they included: sodium hydroxide pellet (NaOH, 98%), hydrochloric acid (HCl) (35.5%), Ammonium hydroxide (NH_4OH, 99.95%), distilled water (H_2O), Sulphuric (VI) acid H_2SO_4 (97 %), Rhodamine blue (RB 95%), and

Glutaraldehyde (GA, 70%). Stock solutions of RB were prepared at 1 gL^{-1}, and diluted using the dilution formula to the desired concentrations before the experiments.
$C_1V_1 = C_2V_2$ where, C_1-concentration of stock solution V_1-volume of stock solution C_2- concentration of dilute solution V_2- volume of dilute solution

Preparation of Irish Potato Peels Powder (IPPP)

Irish Potato peels were collected from Chuka University hotel and washed several times with normal tap water and dried in sun for three days. Dry IPPs were washed with distilled water to remove any dust attached to it. The washed IPPs were dried at 50ºC for 24 hours followed by grinding using electric grinder. The IPPP was sieved using a 250microns mesh size sieve and then stored in air tight plastic bottle for further use. The washing and grinding were done at Chemistry Laboratory, Chuka University.

Preparation of Rice Husks Ash (RHA)

Rice husks were obtained from Mwea Mills at Mwea Market, in Kirinyanga County Kenya and washed comprehensively with distilled water to eliminate any adhering impurities. The washed rice husks were air-dried at room temperature and 100g of it burnt at 700ºC for 2 hours in a furnace. The washing and ashing were done at Chemistry Laboratory, Chuka University.

Preparation of Pure Silica from RHA

10g RHA sample was stirred in 100 ml of 2.5N sodium hydroxide solution and boiled in 250 ml Erlenmeyer flask for 3hours. The 250 ml Erlenmeyer flask was covered with aluminum foil to prevent the complete evaporation of the mixture. The mixture was filtered and the residue washed with 20 ml boiling water into the filtrate for complete extraction of sodium silicate which is in the filtrate.
$SiO_2 + 2NaOH \rightarrow Na_2SiO_3 + H_2O$

The filtrate was cooled down to room temperature and 2.5M H_2SO_4 added until pH 2 was reached. 2M NH_4OH was added to adjust pH to 8.5 and cooling allowed to room temperature. The solution was filtered and the residue dried at 120ºC for 18hours in an oven. The pure silica obtained was weighed on a weighing balance. The preparation of the pure silica was done at chemistry laboratory, Chuka University.
$Na_2SiO_3 + H_2SO_4 \rightarrow SiO2 + Na_2SO4 + H_2O$

Preparation of Nano Silica

10g Pure silica obtained was refluxed with 80 ml 6 N HCl for 4hours and the substrate washed repetitively with distilled water to make it acid free. It was then dissolved in 2.5N NaOH for 1hour on a magnetic stirrer and then concentrated H_2SO_4 was added to adjust pH to 8.5. The precipitated silica was washed repetitively in distilled water until the filtrate was completely alkali free. The product obtained was dried at 50ºC for 48hours in the oven.

Preparation Irish Potatoes Peels Powder- Nano Silica Composite (IPPP–NSC)

5g SNPS were dispersed in 50 ml distilled water in a 250 ml three-necked flask, followed by addition of IPPP and the mixture stirred. The solution was adjusted to PH 8 using ammonia and stirred at 90 °C for 6hours. Glutaraldehyde was added to the mixture and stirring continued for 2hours at 90^0C. The resulting final product (IPPP–NSC) was washed with deionized water and dried

Adsorption Studies

Batch Equilibrium Studies

Batch experiment was carried out with different concentrations of RB solutions from 1mg/l to 5mg/l taken in a 250ml clean Erlenmeyer flasks. A certain amount of adsorbent dose will be mixed with RB solution and kept in an obituary shaker with a speed of 120rpm. Experimental parameters such as, adsorbent dosage, contact time, pH, initial concentration and temperature were investigated by changing one parameter at a time, while other parameters are kept constant. After filtration, the solutions were analyzed by UV-visible spectrophotometer (UV-1800 Shimadzu at Chuka University. The percentage of RB dye removal was calculated by using the following equation.

$$\% \ removal = \frac{Ci - Ce}{Ci} X\ 100$$

Where; Ci - initial (concentration (mg/l), Ce- equilibrium (concentration (mg/l). The adsorption (capacity Qe (mg/g), was obtained from the following equation 9

$$Qe = \frac{Ci - Ce}{M}\ X\ V$$

Where; Qe - adsorbent capacity(mg/g), C_i- initial dye concentration (mg/l), V -volume of the solution(l), M -mass of the adsorbent (g).

III. Results And Discussion

FTIR spectrum of Rice Husk Nanosilica

The figure 1 below, shows strong absorption peaks at 464.86cm^{-1}, 620.14cm^{-1}, 1107.19cm^{-1} indicating the presence of nanostructured SiO_2. The peaks at 464.86cm^{-1} and 620.14cm^{-1} are assigned to bending vibrations of O-Si-O. The peak at 1107.19 cm^{-1} is due to O-Si-O asymmetric stretching vibration while the band at 800cm^{-1} is due to the symmetric stretching vibration of the O-Si-O bond (Farshid *et al.,* 2015). Peak at 1650cm^{-1} corresponds to –OH bending in adsorbed water molecule on the surface of Nano silica (Zhang *et al.,* 2010). Bands from 2106.36 cm^{-1} to 2928.83 cm^{-1} are due to the chemically absorbed water and also due to the silano hydroxyl groups. The moderately sharp peak at 3442.12 cm^{-1} to 3483.59 cm^{-1} is assigned to the stretching frequency of silano hydroxyl group (Majid *et al.,* 2014).

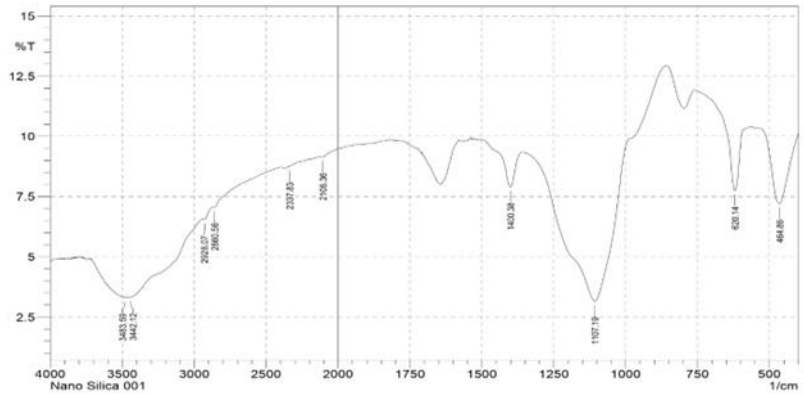

Figure 1. FTIR Spectrum of nanosilica

FTIR spectrum of Irish Potatoes Peels Powder

FTIR spectra in figure 2 below shows peaks at 3223.19 cm^{-1}, 3265.63 cm^{-1} and 3305.17cm^{-1}confirming the presence of free H-bonded and –OH stretching vibration of the hydroxyl group derived from polymers composing the adsorbent such as cellulose and lignin (Ahmed *et al*., 2014). The broadness of the peak is attributed to the existence of water molecules on adsorbent surface. The peak at 2928.07cm^{-1}and 2861.52 cm^{-1} can be attributed to aliphatic C-H bond stretching of methyl and methylene groups in the polymers exiting in IPPP (Farooq *et al*., 2011). Peaks at 1645.35 cm^{-1} to 1629.92cm^{-1} is due to C=O stretching vibration of aldehydes and shows the presence of aromatic compounds in the lignin of IPPP (Bodirlau *et al*., 2009, Khairiraihanna *et al*., 2015). Peaks at 1450 cm^{-1} to 1395.56 cm^{-1}can be assigned to the aromatic C=C stretching mode. Peaks at 1247.03 cm^{-1} to 1153.48 cm^{-1} indicate presence of aryl OH groups. Peaks at 763.84 cm^{-1} to 934.55cm^{-1} can be attributed to -OH and C-O stretching vibrations of the carboxylate group in lignin, hemicellulose, and cellulose (Bansal *et al*., 2009). The FTIR fingerprint region shows that the main component is hemicellulose (Yang *et al*., 2007).

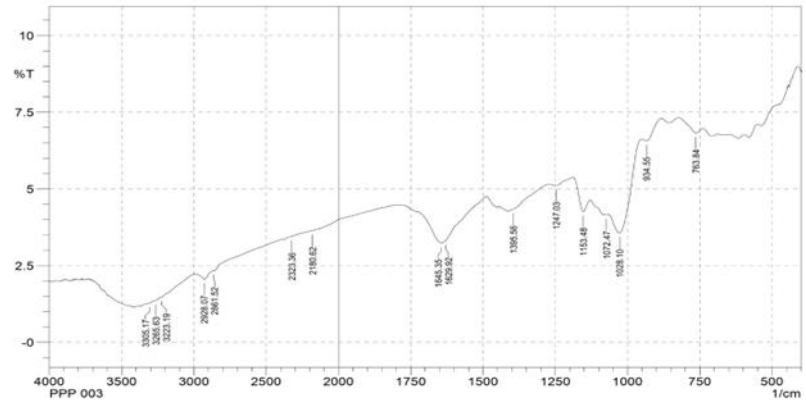

Figure 2. FTIR spectrum of Irish Potatoes Peels Powder

FTIR spectrum of IPPP-NSC

The spectra of the composite shown in figure 3 below shows peaks attributed to functional groups present in Nano silica and Irish potatoes peels powder indicating a composite was effectively synthesized. Strong absorption peaks at 467.76cm^{-1}, 606.64cm^{-1}, 1104.29cm^{-1} indicating the presence of nanostructured SiO_2 (Farshid *et al.,* 2015 and Majid *et al.,* 2014). The peaks at 467.76cm^{-1}and 606.64cm^{-1} are assigned to bending vibrations of O-Si-O. The peak at 1104.29 cm^{-1} is due to O-Si-O asymmetric stretching. Bands from 1953.97 cm^{-1} to 2390.87 cm^{-1} are due to the chemically absorbed water and also due to the silano hydroxyl groups (Zhang *et al.,* 2010). The moderately sharp peak at 3439.23 cm^{-1} to 3442.62 cm^{-1} is assigned to the stretching frequency of silano hydroxyl group. Peak at 2936.75cm^{-} is attributed to aliphatic C-H bond stretching of methyl and methylene groups in the polymers exiting in IPPP (Farooq *et al*., 2011). Peak at 1645.35 cm^{-1} is due to C=O stretching vibration of aldehydes and shows the presence of aromatic compounds in the lignin of IPPP. Peaks at 1381.09cm^{-1}can be assigned to the aromatic C=C stretching mode. Peak at 794.71cm^{-1} can be attributed to -OH and C-O stretching vibrations of the carboxylate group in lignin, hemicellulose, and cellulose (Bansal *et al*., 2009). It is evident that the potatoes peels powder mixed well with Nano silica hence the presence of both functional groups of silica and potatoes peels powder in the spectrum.

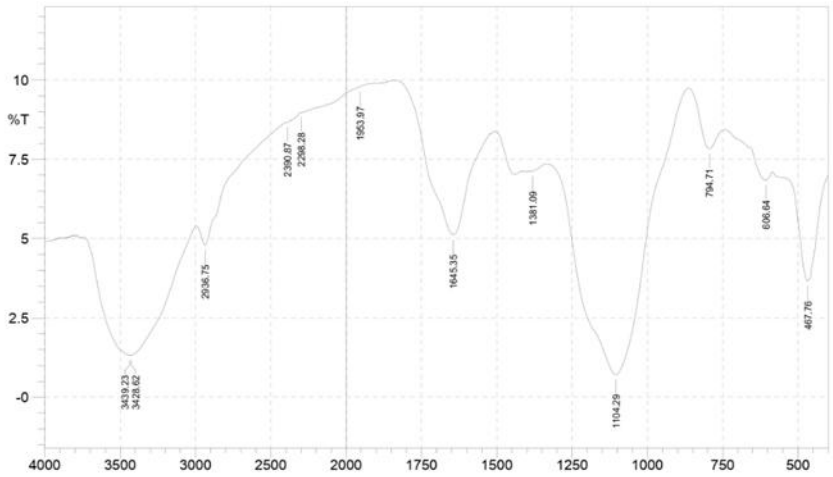

Figure 3. FTIR spectrum of IPPP-NSC

XRD analysis of Composite

XRD diffractograms of composite in Figure 4 showed strong broad peak between 20° and 25° (2θ) that suggested characteristic of amorphous SiO_2 in the composite (Sarkar et al., 2017). There is no significance change in the XRD pattern of the composite since both Irish potatoes peels powder and rice husk nano silica synthesized are amorphous in nature as reported by (Ramezanianpour *et al*., 2009).The X-ray diffraction (XRD) analysis of the Irish potato peel–rice husk nanosilica composite reveals a material structure composed primarily of amorphous silica with minor crystalline content. A distinct sharp peak observed at approximately 2θ ≈ 26.5° is indicative of the (101) plane of crystalline quartz (SiO_2).

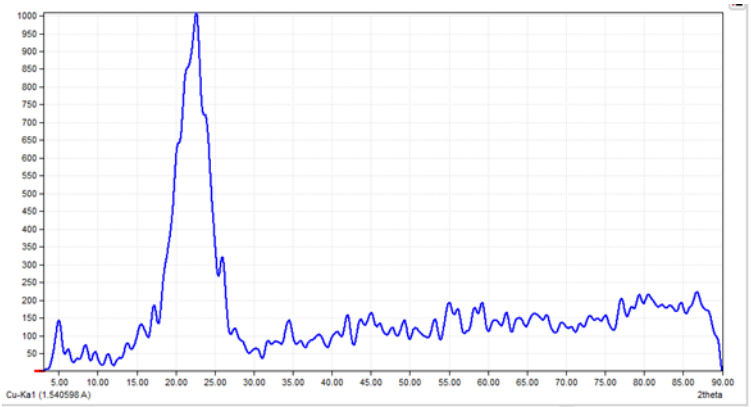

Figure 4.XRD Diffractograms of IPPP-SNC

In contrast, the broad band spanning 15°–35° 2θ is characteristic of amorphous silica, confirming that the majority of the silica present exists in a non-crystalline form. This is a common feature in silica synthesized

from agricultural waste materials, particularly rice husks, under controlled calcination or sol–gel conditions. The amorphous nature of the silica contributes to a high surface area and the presence of reactive silanol groups, which are advantageous in applications such as adsorption, catalysis, and composite reinforcement. The background noise and minor fluctuations observed between 40° and 80° 2θ likely result from the organic matrix contributed by the Irish potato peel component. Potato peels, rich in carbonaceous and polymeric substances such as starch, cellulose, and lignin, typically do not exhibit sharp crystalline peaks in XRD due to their predominantly amorphous and organic nature.

The combination of these two biomass sources has produced a hybrid organic–inorganic material with dominant amorphous features and minor crystalline contributions. The presence of nanosilica provides mechanical and thermal stability, while the organic matter from the potato peels may enhance biocompatibility, functionalization potential, or interfacial bonding in composite applications.These findings align with previous literature on bio-derived silica–organic composites, where XRD patterns typically show a blend of amorphous silica signals with weak crystalline features depending on the synthesis parameters and source materials. The observed structure demonstrates the successful integration of nanosilica from rice husks with biopolymer-rich Irish potato peels, highlighting the potential of this composite as a sustainable, low-cost, and functional material for use in environmental, biomedical, or industrial applications.

BET Adsorption

The BET surface area performed showed a surface area of 100.6328 m^2/g, which is considerably high for biosorbents synthesized from agricultural waste. A higher surface area implies more available active sites for dye molecules, which directly enhances the adsorption efficiency. This is consistent with the high removal rate (97.57%) of Rhodamine Blue (RB) observed during batch adsorption studies. The isotherm in figure 5 below exhibits a characteristic Type IV curve with an H3 hysteresis loop, as per the IUPAC classification, which is indicative of mesoporous materials with slit-shaped pores commonly associated with aggregates of plate-like particles. At low relative pressures (P/Po < 0.3), the quantity of nitrogen adsorbed increases gradually, which corresponds to monolayer-multilayer adsorption on the surface of the composite. The steep rise in the isotherm between P/Po = 0.8 and 1.0 suggests capillary condensation within the mesopores. This behavior is typical of materials possessing a significant proportion of mesopores (2–50 nm in diameter), which are desirable in adsorption applications due to enhanced diffusion and active surface accessibility. The observed hysteresis loop between the adsorption and desorption branches is typical of mesoporous adsorbents and implies a narrow pore size distribution. The H3-type loop further suggests that the pores do not exhibit a well-defined cylindrical geometry but are more likely irregular or slit-shaped, possibly due to the stacking of silica sheets or the layered nature of organic content from Irish potato peels.

Additionally, the Barrett-Joyner-Halenda (BJH) analysis revealed an average pore diameter of 17.93 nm, placing the composite in the mesoporous category. The combination of high surface area, suitable pore size distribution, and abundant functional groups (as seen from FTIR analysis) highlights the potential of IPPP–NSC as an efficient and sustainable adsorbent for dye removal in wastewater treatment.

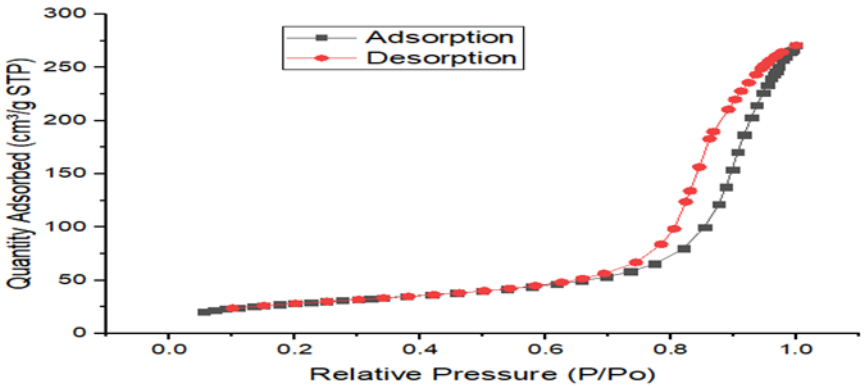

Figure 5. BET-BJH of IPPP-SNC

Adsorption Studies of Rhodamine Blue

Effect of pH on removal of RB

The effect of solution pH on RB sorption was studied using 0.1 g of IPPP-NSC, 1mg l^{-1} dye initial concentration, pH range of 2 to 10 at 25 °C, contact time 80min and shaking speed of 120rpm. The pH is adjusted by adding Hydrochloric acid (0.1 M) or sodium hydroxide (0.1 M), and the results are shown in figure (32) below. In the pH level ranging from 2 to 4, the removal efficiency for RB increased from 86.8 to 97.4%, whereas the pH

level of 4 to 8 made the adsorption capacity of IPPP-NSC to RB relatively stable. However, there were significant declines the removal efficiency of RB corresponding to the increase in pH from 8 to 10 as shown in figure 6. This result was attributed to the change in molecular form of RB at high pH values. Dye molecules becomes difficult to disperse into the pores on the adsorbent surface and thus decrease in adsorption efficiency (Patra *et al*., 2022).

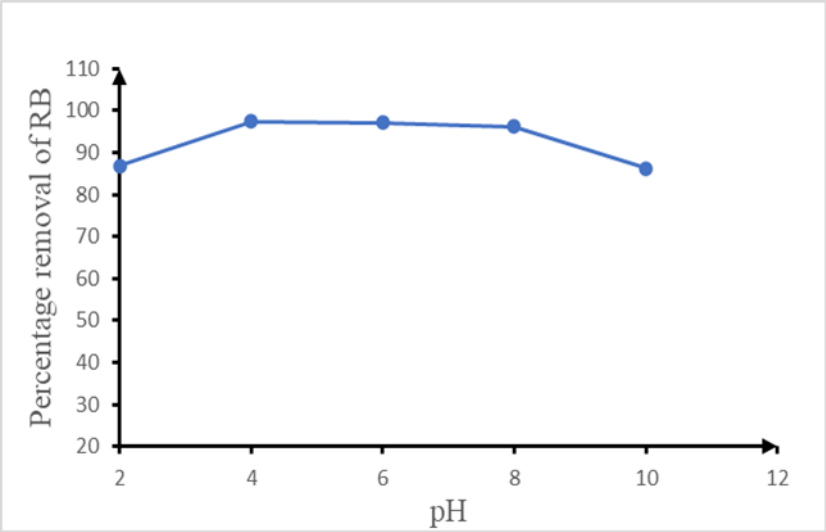

Figure 6. Effect of pH on removal of RB

Effect of contact time on removal of RB

The effect of contact time on the sorption of RB was studied for an initial dye concentration of 1mgl^{-1}, a sorbent mass of 0.1 g, a solution volume of 20 ml, a stirring speed of 120 rpm, and a temperature of 25°C. The effect of contact time on the removal of dye by the IPPP-NSC. It can be observed that the dye uptake increased with time and, at some point in time, reached a constant value where no more dye was removed from the solution as shown in figure7 below. At this point, the amount of dye being adsorbed onto the adsorbent was in a state of dynamic equilibrium with the amount of dye desorbed from the sorbent. The time required to attain this state of equilibrium was termed the equilibrium time and the amount of dye adsorbed at the equilibrium time reflected the maximum dye adsorption capacity of the sorbent under these particular conditions (Errais *et al*., 2011). The contact time necessary to reach equilibrium is 80 min. The rapid sorption observed during the first 80 min is due to the abundant availability of active sites on the IPPP-NSC surface, and with the gradual occupancy of these sites, the sorption becomes less efficient (Errais *et al*., 2011).

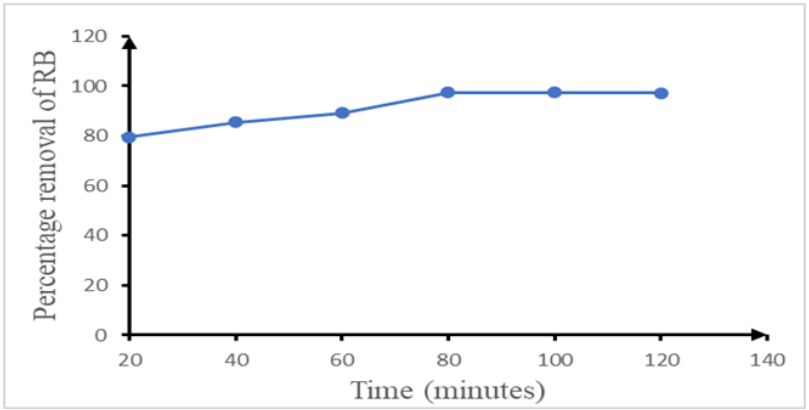

Figure 7. Effect of contact time on removal of RB

Effect of Adsorbent dosage on removal of RB

The experiment studying the effects of applied IPPP-NSC doses on RB adsorption was arranged at different dosages ranging from 0.1 to 0.5 mg/20 mL, initial RB concentration of 1 mg/L, solution pH of 4, temperature of 25^{0}C, a stirring speed of 120 rpm and contact time of 80 min. The results for the dye uptake using various amounts of IPPP-NSC are shown in the figure 8. The equilibrium dye uptake capacity (qe) was found to decrease with an increase in the dosage of the adsorbent, and was best when using 0.1 g. Thus, 0.1 g of adsorbent was selected as the optimum adsorbent dosage.

The decrease in dye uptake value was due to the splitting effect of the flux (concentration gradient) between the adsorbate and adsorbent. It can be explained by the interaction between the adsorbent molecules which leads to the desorption of RB molecules from the narrow sites of the adsorbent and on the other hand the reduction of the specific surfaces due to the formation of an aggregation of the particles of adsorbents (Pourjavadi *et al*., 2016). The decrease could also be explained by the unsaturation of the adsorption sites. These results show that for an increase in each adsorbent dosage, the adsorbent sites available upon the dye molecules also increase and consequently poor adsorption. Another consequence is the reduction of active sites at the surface of the absorbents and also the matter rate transfer of the dye at the surface of the absorbents, this means that the quantity of the dye adsorbed per unit mass of adsorbent has it limit with the adsorbent dosage (Ma *et al.,* 2012).

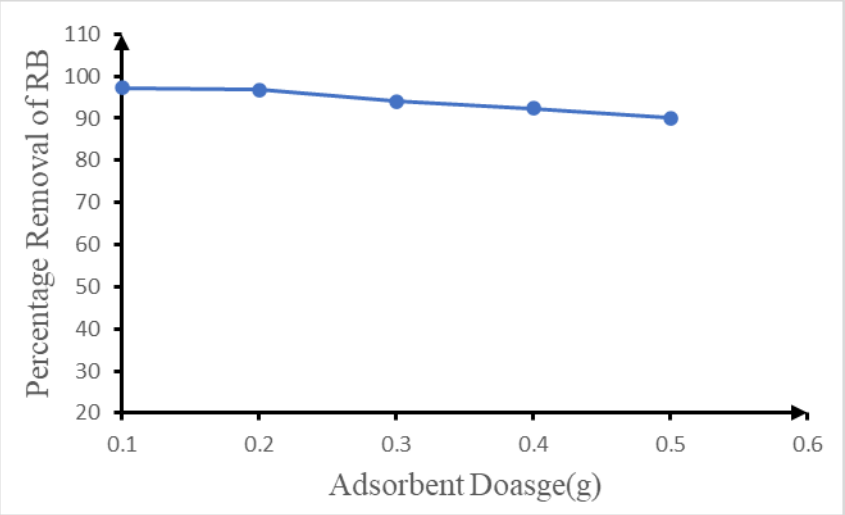

Figure 8. Effect of Adsorbent dosage on removal of RB

Effect of temperature on removal of RB

To observe the effect of temperature, adsorption studies of initial RB concentration of 1 mg/L, solution pH of 4, a stirring speed of 120 rpm and contact time of 80 min were performed at three different temperatures: 25 35, 45, and 55 °C. The results indicate that when the temperature increased from 25^0 C to 55^0 C, the removal efficiency of RB onto IPPP-NSC decreased from 97.47% to 91.26% (figure 9). This may be explained that the adsorption process is exothermic in nature (Boumchita *et al.*, 2016).

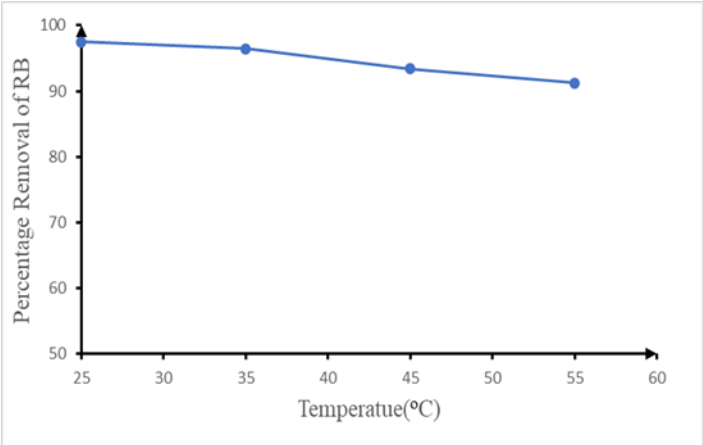

Figure 9. Effect of temperature on removal of RB

Effect of initial dye concentration on removal of RB

The data indicate that percentage of dye removed decreases with increase in the initial concentration of dye (figure 10). As at lower concentration, maximum dye particles in solution occupy available binding sites on adsorbent, which results in better adsorption. But at higher concentration, the available sites on the adsorbent become limited and there is no further adsorption (Sulyman *et al*., 2020). In case of adsorption capacity, the adsorption capacity increases with increase in initial dye concentration because the increase in initial dye concentration enhances the interaction between dye and adsorbent (Goswami and Phukan, 2017).

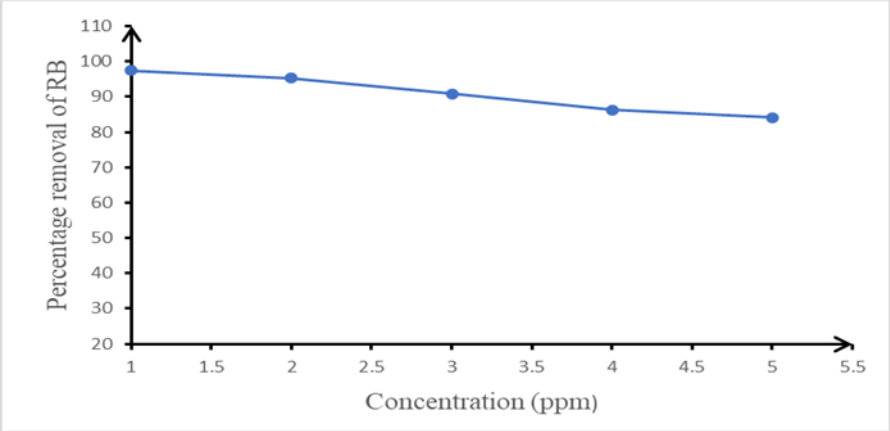

Figure 10. Effect of initial dye concentration on removal of RB

Adsorption Isotherms

The suitability of isotherm equations for the prediction of the pattern of adsorption is very important for industrial design and application. Equilibrium adsorption data for the degradation of RB by IPPP-NSC were studied using the Langmuir and Freundlich models. A linearized form of Langmuir equation plot for RB is shown in figure 16 and the Freundlich equation in figure 17. The regression coefficients of the Langmuir and Freundlich equations are given table 1. The Freundlich isotherm fitted better for the degradation of RB, with an R^2=0.99617 compared to Langmuir values of R^2=0.98752. This suggests that the adsorption process was not on uniform sites but the uptake capacity of the adsorbent was on a heterogeneous surface. The observed pattern of adsorption was similar to the study of (Inyinbor *et al*., 2016) where it was observed that RB removal was more similar to the Freundlich isotherm model.

Table 1 Langmuir and Freundlich constants

	Langmuir			Freundlich		
Sample	Q_{max} (mg/g)	K_L (Lmg^{-1})	R^2	1/n	K_F (mg/g)	R^2
RB	0.9371	6.972	0.98752	0.40812	0.60981	0.99617

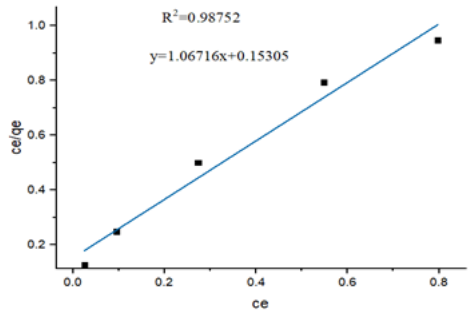

Figure 16. Langmuir isotherm of RB

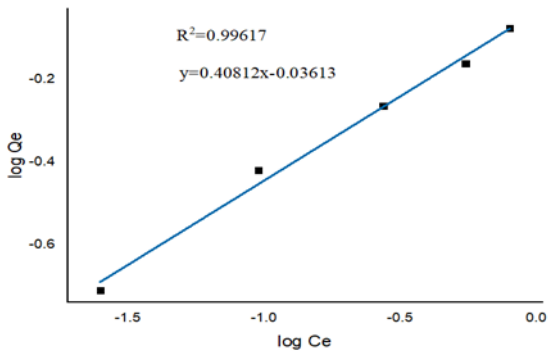

Figure 17. Freundlich isotherm of RB

Adsorption Kinetics

The evaluation of the factors of the two kinetic models were investigated and presented in table 3. The plots are shown in (figure 18) t/qt against t and (figure 19) ln (q_e–q_t) against t. The kinetics of the adsorption of RB by the composite were characterized by the pseudo second order in terms of the closeness of the correlation coefficient to 1, indicating that the kinetics of adsorption of RB can better be explained by the pseudo second order model. It was observed from the data that the initial adsorption rate (mins) increases with the increase in the initial adsorbate concentration, suggesting that RB adsorption was influenced by mass transfer (Fu *et al.,* 2015). By implication, the dye molecule was adsorbed by reaching the surface of the adsorbent at a very short equilibrium time. This may be possibly attributed to the active sites and functional groups present on the surface of the adsorbent. Since the kinetics of the uptake capacity of the composite obeyed the pseudo second order model, it is therefore considered that RB removal was a rate controlling mechanism as a result of the formation of a chemisorptive bond between the adsorbent and the adsorbate (shan *et al.,* 2015).

Table *2* Adsorption kinetics of RB

	Pseudo first order kinetic model			Pseudo second order kinetic model		
Sample	K_1 (1/min)	qe	R^2	K_2(g/mg.min)	qe	R^2
RB	0.1153	0.1301	0.67458	64.387	0.20774	0.9989

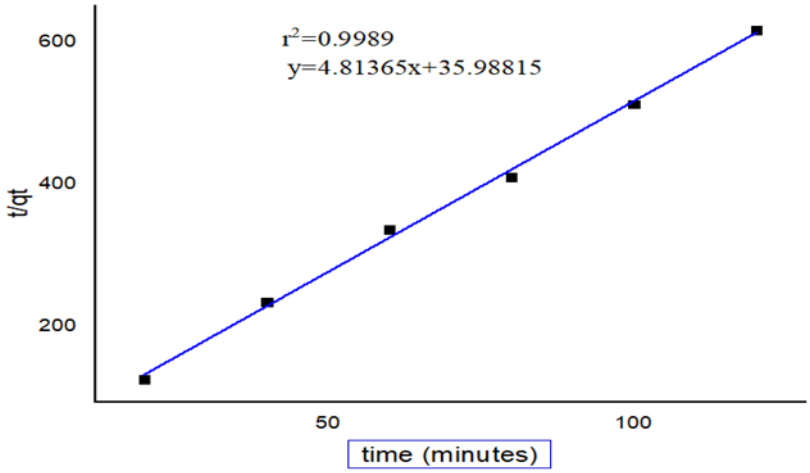

Figure 18. Pseudo second order kinetic model of RB

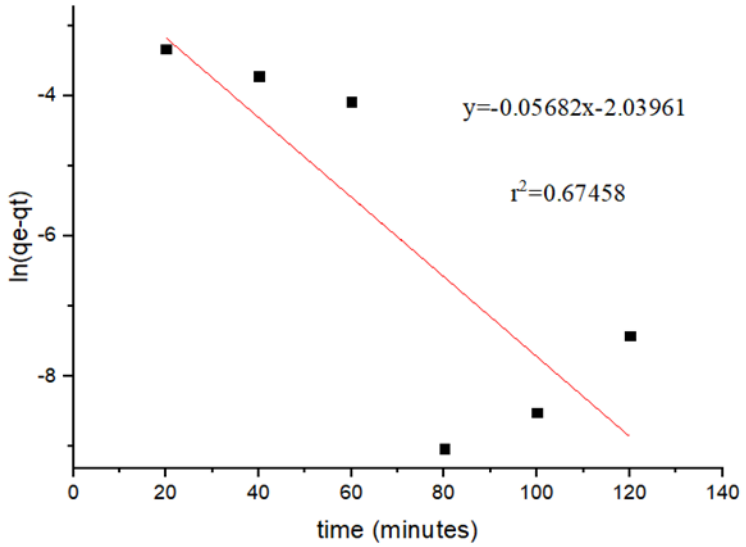

Figure 19. Pseudo first order kinetic of RB

IV. Conclusions

The use of IPPP and RHNS to synthesize a composite IPPP-NSC was ascertained. The synthesized composite was subjected to a variety of characterization tests. Fourier transform infrared spectra of the IPPP and Nano silica show that they contain functional groups on their surface. When they are combined to form composite the number of active groups on the solid support surface increases such as -OH, C-H, C=C, C-O, C=O, Si-OH, O-Si-O, which are responsible for adsorption of Rhodamine blue as evidenced in the FTIR spectrum. XRF analysis of the composite revealed silica formed larger percentage in the composite ascertaining the ratio in which RHNS and IPPP were mixed (4:1). BJH surface characterization showed the composite had surface area of 100.6328m^2/g with single point surface area at P/Po=0.300844548 being 97.4036m^2/g. The average pore diameter was found to be 179.345 Å. The diffraction pattern of the particles showed a diffuse pattern which indicative of amorphous phase and supported by XRD patterns.

The adsorption capacity of Rhodamine blue by the composite was optimum at pH 4, adsorbent dosage 0.1g, initial concentration 1mg/L and agitation speed of 240 rpm. The equilibrium between the adsorbate in the solution and the adsorbent surface was attained in about 80 minutes for Rhodamine blue and at an optimum temperature of 298 K. Efficiency of the adsorbents toward removal of Rhodamine blue increases with adsorbent dose up to 0.1 g. The removal efficiency of RB was found to be 97.57% at optimum conditions. RB removal best fitted Freundlich isotherm in the composite adsorbent used with adsorption capacity of 1.0868mg/g. Higher adsorption capacity is associate to higher surface area, fineness and higher concentration of vacant sites that can be achieved in activated materials

References

[1] Bansal, R., Kiku, D., & Yaron, A. (2009). An Empirical Evaluation Of The Long-Run Risks Model For Asset Prices (No. W15504). National Bureau Of Economic Research.

[2] Benjelloun, Y., Miyah, Y., Idrissi, M., Boumchita, S., Lahrichi, A., Ouali, L. A., & Zerrouq, F. (2016). Study Of Catalytic Performance For The Oxidation Of Methylene Blue Using Mno-Clay Catalyst With H2O2. J Mater Environ Sci, 7(1), 9-17.

[3] Bodirlau, R., & Teaca, C. A. (2009). Fourier Transform Infrared Spectroscopy And Thermal Analysis Of Lignocellulose Fillers Treated With Organic Anhydrides. Rom. J. Phys, 54(1-2), 93-104.

[4] Brandstätter, E., Gigerenzer, G., & Hertwig, R. (2008). Risky Choice With Heuristics: Reply To Birnbaum (2008), Johnson, Schulte-Mecklenbeck, And Willemsen (2008), And Rieger And Wang (2008).

[5] Carneiro, P. A., Umbuzeiro, G. A., Oliveira, D. P., & Zanoni, M. V. B. (2010). Assessment Of Water Contamination Caused By A Mutagenic Textile Effluent/Dyehouse Effluent Bearing Disperse Dyes. Journal Of Hazardous Materials, 174(1-3), 694-699.

[6] Da Silva, C. M., Da Silva, D. L., Modolo, L. V., Alves, R. B., De Resende, M. A., Martins, C. V., & De Fátima, Â. (2011). Schiff Bases: A Short Review Of Their Antimicrobial Activities. Journal Of Advanced Research, 2(1), 1-8.

[7] Dasgupta, N., Scircle, M. M., & Hunsinger, M. (2015). Female Peers In Small Work Groups Enhance Women's Motivation, Verbal Participation, And Career Aspirations In Engineering. Proceedings Of The National Academy Of Sciences, 112(16), 4988-4993.

[8] Ellis, R. (2006). Current Issues In The Teaching Of Grammar: An SLA Perspective. TESOL Quarterly, 40(1), 83-107.

[9] Errais, E., Duplay, J., Darragi, F., M'Rabet, I., Aubert, A., Huber, F., & Morvan, G. (2011). Efficient Anionic Dye Adsorption On Natural Untreated Clay: Kinetic Study And Thermodynamic Parameters. Desalination, 275(1-3), 74-81.

[10] Farooq, M. S., Chaudhry, A. H., Shafiq, M., & Berhanu, G. (2011). Factors Affecting Students' Quality Of Academic Performance: A Case Of Secondary School Level. Journal Of Quality And Technology Management, 7(2), 1-14.

[11] Ferraz, E. R. A., Umbuzeiro, G. A., De-Almeida, G., Caloto-Oliveira, A., Chequer, F. M. D., Zanoni, M. V. B., ... & Oliveira, D. P. (2011). Differential Toxicity Of Disperse Red 1 And Disperse Red 13 In The Ames Test, Hepg2 Cytotoxicity Assay, And Daphnia Acute Toxicity Test. Environmental Toxicology, 26(5), 489-497.

[12] Golka, K., Kopps, S., & Myslak, Z. W. (2004). Carcinogenicity Of Azo Colorants: Influence Of Solubility And Bioavailability. Toxicology Letters, 151(1), 203-210.

[13] Gollub, J., & Benson, S. V. (1980). Many Routes To Turbulent Convection. Journal Of Fluid Mechanics, 100(3), 449-470.

[14] Goswami, M., & Phukan, P. (2017). Enhanced Adsorption Of Cationic Dyes Using Sulfonic Acid Modified Activated Carbon. Journal Of Environmental Chemical Engineering, 5(4), 3508-3517.

[15] Khairiraihanna, J., Norasikin, S., Song, S., & Hanapi, M. (2015). Adsorption Equilibrium And Kinetics Of Elemental Mercury Onto Coconut Pith. Journal Of Environmental Science And Technology, 8(2), 74-82.

[16] Kim, H. Y., Lee, H. J., Chang, Y. J., Pichavant, M., Shore, S. A., Fitzgerald, K. A., ... & Umetsu, D. T. (2014). Interleukin-17–Producing Innate Lymphoid Cells And The NLRP3 Inflammasome Facilitate Obesity-Associated Airway Hyperreactivity. Nature Medicine, 20(1), 54-61.

[17] Kolpin, D. W., Furlong, E. T., Meyer, M. T., Thurman, E. M., Zaugg, S. D., Barber, L. B., & Buxton, H. T. (2002). Pharmaceuticals, Hormones, And Other Organic Wastewater Contaminants In US Streams, 1999− 2000: A National Reconnaissance. Environmental Science & Technology, 36(6), 1202-1211.

[18] Ma, C. S., Deenick, E. K., Batten, M., & Tangye, S. G. (2012). The Origins, Function, And Regulation Of T Follicular Helper Cells. Journal Of Experimental Medicine, 209(7), 1241-1253.

[19] Majid, A., Dawson, J., Lees, K. R., Tyrrell, P. J., & Smith, C. J. (2014). Detection Of Atrial Fibrillation After Ischemic Stroke Or Transient Ischemic Attack: A Systematic Review And Meta-Analysis. Stroke, 45(2), 520-526.

[20] Modi, K., Paterek, T., Son, W., Vedral, V., & Williamson, M. (2010). Unified View Of Quantum And Classical Correlations. Physical Review Letters, 104(8), 080501.

[21] Pourjavadi, A., Nazari, M., Kabiri, B., Hosseini, S. H., & Bennett, C. (2016). Preparation Of Porous Graphene Oxide/Hydrogel Nanocomposites And Their Ability For Efficient Adsorption Of Methylene Blue. RSC Advances, 6(13), 10430-10437.

[22] Pradhan, B., Nayak, R., Patra, S., Bhuyan, P. P., Behera, P. K., Mandal, A. K., ... & Jena, M. (2022). A State-Of-The-Art Review On Fucoidan As An Antiviral Agent To Combat Viral Infections. Carbohydrate Polymers, 119551.

[23] Raheem, A. R., Vishnu, P. A. R. M. A. R., & Ahmed, A. M. (2014). Impact Of Product Packaging On Consumer's Buying Behavior. European Journal Of Scientific Research, 122(2), 125-134.

[24] Ramezanianpour, A. A., Mahdikhani, M., & Ahmadibeni, G. H. (2009). The Effect Of Rice Husk Ash On Mechanical Properties And Durability Of Sustainable Concretes.
[25] Robinson, T., Mcmullan, G., Marchant, R., & Nigam, P. (2001). Remediation Of Dyes In Textile Effluent: A Critical Review On Current Treatment Technologies With A Proposed Alternative. Bioresource Technology, 77(3), 247-255.
[26] Saratale, R. G., Saratale, G. D., Chang, J. S., & Govindwar, S. P. (2011). Bacterial Decolorization And Degradation Of Azo Dyes: A Review. Journal Of The Taiwan Institute Of Chemical Engineers, 42(1), 138-157.
[27] Sarkar, P., Moyez, S. A., Dey, A., Roy, S., & Das, S. K. (2017). Experimental Investigation Of Photocatalytic And Photovoltaic Activity Of Titania/Rice Husk Crystalline Nano-Silica Hybrid Composite. Solar Energy Materials And Solar Cells, 172, 93-98.
[28] Schwarzenbach, R. P., Egli, T., Hofstetter, T. B., Von Gunten, U., & Wehrli, B. (2010). Global Water Pollution And Human Health. Annual Review Of Environment And Resources, 35, 109-136.
[29] Sulyman, A. O., Igunnu, A., & Malomo, S. O. (2020). Isolation, Purification And Characterization Of Cellulase Produced By Aspergillus Niger Cultured On Arachis Hypogaea Shells. Heliyon, 6(12), E05668.
[30] Vogl, T. J., Farshid, P., Naguib, N. N., Zangos, S., Bodelle, B., Paul, J., ... & Nour-Eldin, N. E. A. (2015). Ablation Therapy Of Hepatocellular Carcinoma: A Comparative Study Between Radiofrequency And Microwave Ablation. Abdominal Imaging, 40, 1829-1837.
[31] Wang, J., Su, Y., Lv, S. W., & Sun, L. H. (2022). The Efficient Removal Of Diclofenac Sodium And Bromocresol Green From Aqueous Solution By Sea Urchin-Like Ni/Co-BTC Bimetallic Organic Framework: Adsorption Isotherms, Kinetics And Mechanisms. New Journal Of Chemistry, 46(38), 18374-18383.
[32] Yang, H., Yan, R., Chen, H., Lee, D. H., & Zheng, C. (2007). Characteristics Of Hemicellulose, Cellulose And Lignin Pyrolysis. Fuel, 86(12-13), 1781-1788.
[33] Zhang, Y., Du, T., An, X., Tu, Z., & Zhang, G. (2010). Study On Ce-Doped Nonstoichiometric Nanosilica For Promoting Properties Of Polysulfone Membranes. Chemical Engineering & Technology: Industrial Chemistry-Plant Equipment-Process Engineering-Biotechnology, 33(4), 676-681.